



The Relationship between Sea Surface Temperature and Chlorophyll-*a* Concentration in Arabian Sea

Umair Bin Zamir*, Hina Masood*, Nelofer Jamil**, Anila Bahadur***, Muniza Munir***, Palwasha Tareen***, Nafisa Kakar*** and Humaira Ashraf****

*Department of Geography, University of Karachi, Karachi Pakistan.

**Department of Chemistry, Sardar Bahadur Khan Women University, Quetta, Pakistan.

***Department of Environmental Science, Sardar Bahadur Khan Women University, Quetta, Pakistan

****Department of Computer Science, Sardar Bahadur Khan Women University, Quetta, Pakistan

(Corresponding author: Hina Masood)

(Received 12 August, 2015, Accepted 09 October, 2015)

(Published by Research Trend, Website: www.researchtrend.net)

ABSTRACT: This study examine the association between sea surface temperature (SST) and chlorophyll-*a* (Chl-*a*) by using OC3M algorithm across the Arabian Sea. Investigating the affiliation between SST and Chl-*a* helps in understanding the ocean yields pattern. A multi temporal dataset from June 2013 to May 2014 MODIS Aqua satellite-derived ocean chlorophyll concentration and sea surface temperature is used for analyzing the changing trends by using cubic regression analysis. This study also attempts to monitor the monthly variation in chlorophyll-*a* pattern across the Arabian Sea. A typical GIS and RS techniques are used for depicting the temporal variation and finding the relationship between chlorophyll-*a* with sea surface temperature (SST).

Keywords: Chlorophyll-*a* concentrations, sea surface temperature, MODIS, remote sensing, Arabian Sea.

INTRODUCTION

Remote sensing is a powerful aid to monitor Ocean color that helps in collecting information about the ingredients of sea water like phytoplankton pigments, suspended sediments etc. Mapping of Sea and detection of constituents by using space-borne platform helps in routine monitoring of temporal variation of Chl-*a*. Monitoring the trends of marine ecosystem productivity is the major concerned from past few decades by different scientific societies and in many international publications (Behrenfeld *et al.*, 2006; Boyce, Lewis, & Worm, 2010; Doney, 2006; Piontkovski & Castellani, 2009; Worm, Sandow, Oschlies, Lotze, & Myers, 2005). The potential of oceanic ecosystem in terms of yield is often dependent upon the concentration of (chlorophyll-*a*) or in oceanic remote sensing presence of (chlorophyll-*a*) is considered as a representation of the phytoplankton whilst this indicator of productivity should be applied carefully (Hayward & Venrick, 1982; Longhurst, 1998). Generally (chlorophyll-*a*) is a crucial pigment and a requisite for photosynthesis in phytoplankton. Phytoplankton is the source of food for the marine life and monitoring chlorophyll-*a* data is useful for understanding the ocean productivity pattern. Chl-*a* is the most common pigment of marine phytoplankton therefore it is used as an indicator for the existence of phytoplankton (Li *et al.*, 2002). The blue-green wavelengths of light spectrum are a unique spectral characteristic of Chl-*a* that has made it visible from remote sensing.

Mapping chlorophyll-*a* is significant in the fishing industry but earlier it was difficult, time consuming and an expensive deal to monitor chlorophyll-*a* concentration over a large area by the traditional means of sampling, Satellite remote sensing is an aid in order to resolve this issue of spatial coverage by providing global snap shot of chl-*a* with multi temporal data. Chl-*a* from satellite sensors helps in examining the oceanic environment without in-situ sampling. The association of ocean colors and Chl-*a* concentration has been studied for several decades (Clark, 1981; Gordon *et al.*, 1983). Globally annual or interannual trends of chlorophyll-*a* are observed and monitor by using Remote Sensing technology. Remote sensing data used in this study is Moderate Resolution Imaging Spectroradiometer (MODIS-Aqua) for the period of June 2013 to May 2014 for both Chl-*a* and SST.

Study Area

The Arabian Sea is geographically located in the western part of north Indian Ocean and is surrounded by India on the east, Arabian Peninsula on the west, Pakistan and Iran on the north and Somalia on the southwest (Fig.1). This warm water zone is having a great potential for the fishing industry because of variety of fish resources. The Arabian Sea is having some distinctive physiognomies in the form of seasonally reversing monsoon winds. In summer from June to September the movement of wind is from south west and in winter from November to February it follows the northeasterly pattern.

This seasonal oscillation is somehow responsible for the upwelling and distribution of chlorophyll-*a* across the Arabian Sea. Similarly the surface currents of this region have unique characteristics (Banse & English, 2000; Varkey, Murty & Suryanarayana, 1996). There are different factors responsible for the chlorophyll-*a*

concentration during the south west monsoon and Northeast monsoon reported by different studies (Bhattathiri *et al.*, 1996; Lévy *et al.*, 2007; Wiggert, Hood, Banse, & Kindle, 2005). However there is a spatial and temporal variation of productivity is also found in Arabian Sea (Lévy *et al.*, 2007).

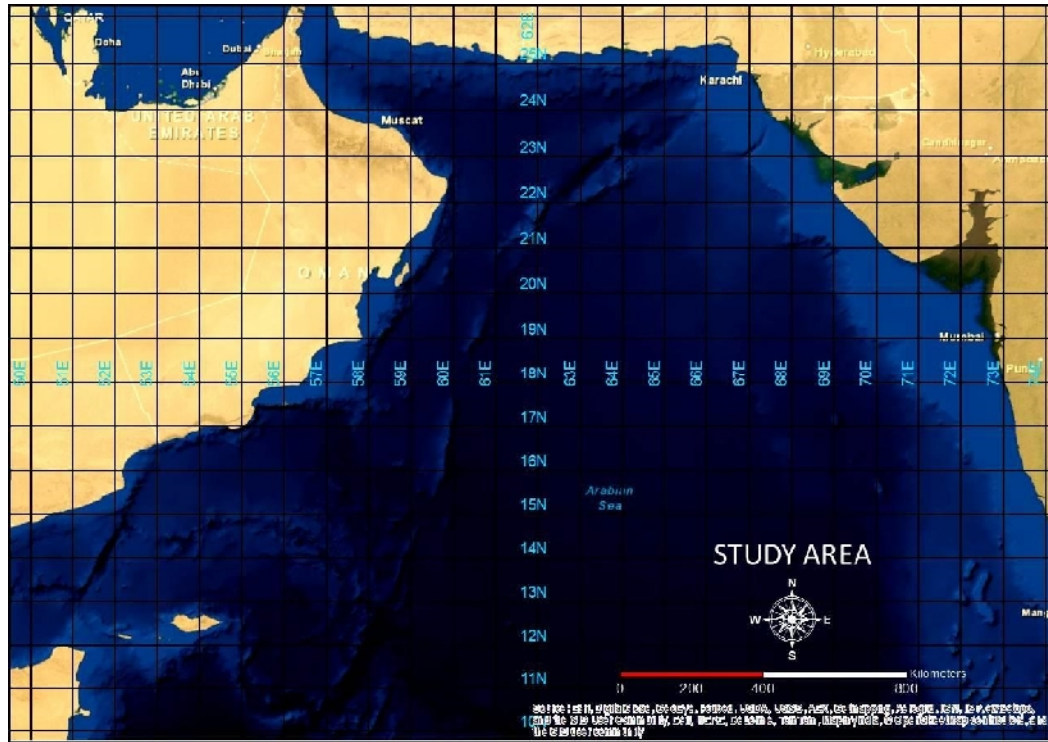


Fig. 1. The Study Area.

MATERIALS AND METHODS

Moderate Resolution Imaging Spectroradiometer Satellite (MODIS-Aqua) monthly data of chl-*a* and SST from June 2013 to May 2014 across the Arabian Sea is used in order to explore the Fig.1. The Study Area association among Chl-*a* and SST. This time series data is obtained from NASA Ocean Colors.

The dataset used is Ocean Color Level-2 browse product which are produced and distributed by the NASA Goddard Space Flight Center's Ocean Color Data Processing System (OCDPS).

Chl-*a* is derived from OC3M algorithm which is generically represented as:

$$\log_{10}(\text{chl}) = a_0 + a_1 * x + a_2 * x^2 + a_3 * x^3 + a_4 * x^4,$$

where $x = \log_{10}(\text{Rrs band ratio})$.

Where, the Rrs band ratio for OC3 algorithm is: Rrs443 / Rrs551 and Rrs488 / Rrs551 (MODIS ocean bands).

The Image or data acquisition is the most important step for any remote sensing based study. The dataset obtained is HMODIST Level-2 data where HMODIST is the sensor name. The software

used for deriving this product is 12gen version 6.7.0. This product is produced and distributed by NASA Goddard Space Flight Center's Ocean Color Data Processing System (OCDPS). The dataset is downloaded from (<http://oceandata.sci.gs.nasa.gov>). The detail specification or metadata are shown in Table 1. The obtained data for Chl-*a* and SST is in HDF format which is reprojected to WGS1984 and converted into TIFF format. Furthermore files are exported into Erdas Imagine image processing software where atmospheric correction is applied (where required) to MODIS data for avoiding the varying illumination conditions and to get the best possible spectral behavior. For delineating the land water boundary land masking is done. The Image obtained is further exported in ArcGIS for the geo processing purpose; the objective is to extract the values from Chl-*a* image and SST, for this to achieve the raster of Chl-*a* is converted into point and the values of the pixels of SST at same spatial location are also retrieved so that pixel versus pixel contrast is obtained.

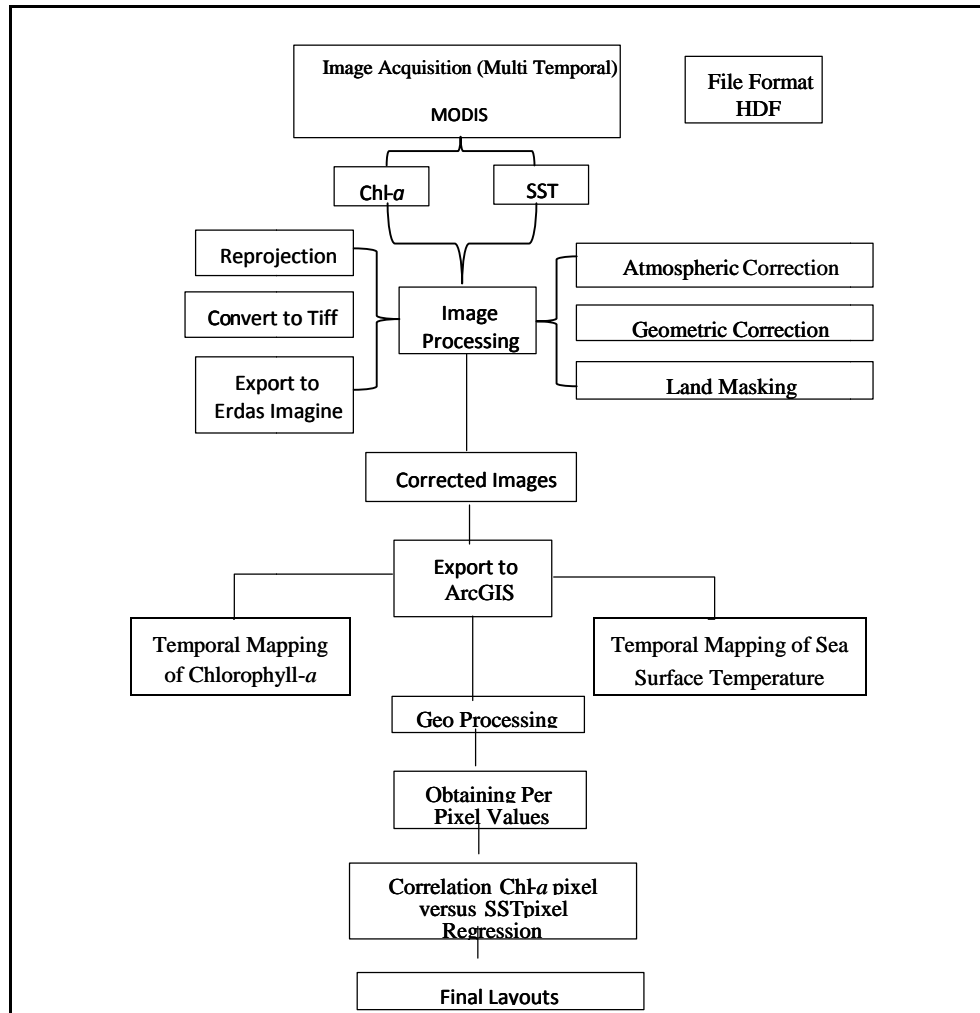


Fig. 2. Methodological Framework.

After retrieving the values the attributes are converted into dbf format and export to Minitab (Statistical software) for performing the correlation and regression analysis. Finally all the results are mapped by using ArcGIS 10.1 software.

RESULTS AND DISCUSSION

A. Chlorophyll-a

There are 12 scenes from June 2013 to May 2014 of Chlorophyll-a which were processed. The general statistics for Chl-a are appeared in Table 2 and Fig. 3 including total number of pixels represents chlorophyll-a presence, minimum and maximum value of Chl-a etc. Similarly 12 scenes of sea surface temperature (SST) were processed and SST general statistics are appeared in (Table 3 and Fig. 4).

The pixel counts for SST and Chl-a are of same locations therefore the counts of pixel for Chl-a and SST are same. There are more pixel counts found in the month of April (Fig. 5) for Chl-a which shows that there are well distributed chlorophyll-a pigments are found in April but it does not signified that the chlorophyll-a values are also maximum or at their peak in this month. In the Table 2 Chl-a pixels counts are representing the chlorophyll-a traces found in the different months. The number of chlorophyll-a traces are high in the month of January, February, March but a sharp increase in chl-a traces in the month of April. A drastic decline is appeared in the month of May while it stands till the month of August. In September traces of chl-a again starts increasing within the study area and it keeps on increasing till December.

Table 1: MODIS -Aqua(Metadata).

Name	Value	Type
Title	HMODIST Level-2 Data	ascii
Sensor_Name	HMODIST	ascii
Product_Name	T2014001062000.L2_LAC_OC (Variable)	ascii
Software_Name	l2gen	ascii
Software_Version	6.7.0	ascii
Processing_Version	2013	ascii
Conventions	CF-1.6	ascii
institution	NASA Goddard Space Flight Center, Ocean Ecology Laboratory, Ocean Biology Processing Group	ascii
license	http://science.nasa.gov/earth-science/earth-science-data/data-information-policy/	ascii
naming_authority	gov.nasa.gsfc.sci.oceandata	ascii
date_created	20140104T040112Z	ascii
keywords_vocabulary	NASA Global Change Master Directory (GCMD) Science Keywords	ascii
stdname_vocabulary	NetCDF Climate and Forecast (CF) Metadata Convention	ascii
creator_name	NASA/GSFC/OBPG	ascii
creator_email	data@oceancolor.gsfc.nasa.gov	ascii
creator_url	http://oceandata.sci.gsfc.nasa.gov	ascii
project	Ocean Biology Processing Group (NASA/GSFC/OBPG)	ascii
publisher_name	NASA/GSFC/OBPG	ascii
publisher_url	http://oceandata.sci.gfc.nasa.gov	ascii
publisher_email	data@oceancolor.gsfc.nasa.gov	ascii
processing_level	L2	ascii
cdm_data_type	swath	ascii
Orbit_Node_Longitude	60.548717	float32
Orbit_Number	74675	int32
Node_Crossing_Time	2.014E+18	ascii
Processing_Time	2.014E+15	ascii
Mask_Names	ATMFAIL,LAND,CLDICE,HILT	ascii
Number_of_Bands	16	int32
Number_of_Scan_Lines	2030	int32
Pixels_per_Scan_Line	1354	int32
Scene_Center_Scan_Line	1015	int32
Number_of_Scan_Control_Points	2030	int32
Number_of_Pixel_Control_Points	1354	int32
Earth-Sun_Distance_Correction	1.034246325	float64
_History	Direct read of HDF4 file through CDM library	ascii
HDF4_Version	4.2.9 (HDF Version 4.2 Release 9, February 7, 2013)	ascii

Table 2: Statistics - Chlorophyll-a.

Month	Chl-a Pixel Counts	Minimum	Maximum	Sum	Mean	Standard Deviation
January2014	897605	0	0.391	129107.5	0.143836	0.064451
February 2014	817001	0.003	0.441	151854.5	0.185868	0.056599
March 2014	748542	0.028	0.432	62477.18	0.083465	0.040455
April 2014	921834	0.026	4.705	1136806	1.233201	0.585514
May 2014	44995	0.055	0.242	5874.964	0.130569	0.038219
June 2013	279987	0.016	0.486	33171.93	0.118477	0.046097
July 2013	574	0.063	0.472	231.527	0.403357	0.086748
August 2013	5446	0.048	0.484	1328.085	0.243864	0.083933
September 2013	234156	0.028	0.513	46069.16	0.196746	0.047544
October 2013	443184	0.029	0.466	68256.06	0.154013	0.05091
November 2013	658056	0.014	0.401	111559.6	0.169529	0.053107
December 2013	708509	0.028	0.324	76175.68	0.107515	0.043823

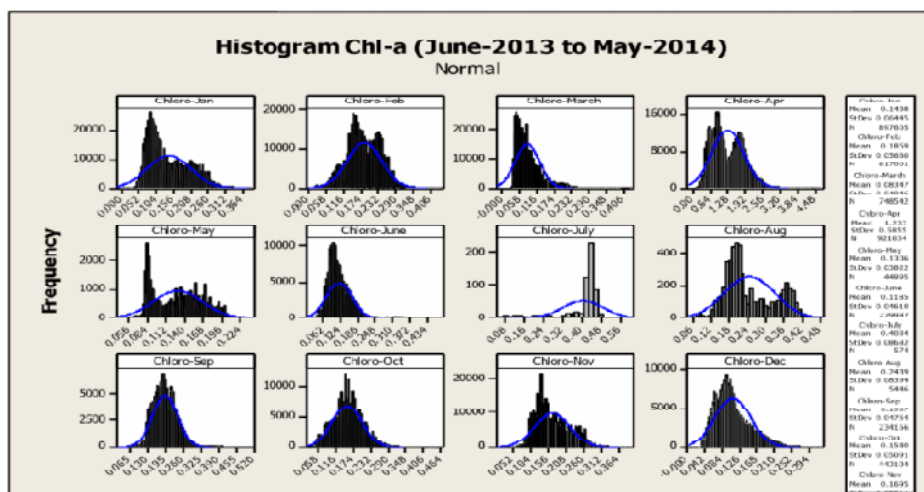


Fig. 3. Histogram Chlorophyll-a.

Table 3: Statistics - Chlorophyll-a.

Month	SST-Pixel Count	Minimum	Maximum	Sum	Mean	Standard Deviation
January2014	897605	12	28	22066877	24.58417	1.039496
February 2014	817001	17	28	19463151	23.82268	1.39789
March 2014	748542	20	29	18133862	24.22558	1.280397
April 2014	921834	22	38	24799484	26.90233	1.687275
May 2014	44995	25	31	1291258	28.69781	1.026119
June 2013	279987	3	46	8262593	29.51063	0.981478
July 2013	574	22	30	15602	27.18119	0.709759
August 2013	5446	23	28	144062	26.45281	0.582423
September 2013	234156	15	35	6343462	27.09075	1.104852
October 2013	443184	17	30	12182405	27.48837	0.92873
November 2013	658056	0	31	16084594	24.44259	9.889967
December 2013	708509	22	29	18643143	26.31321	0.65498

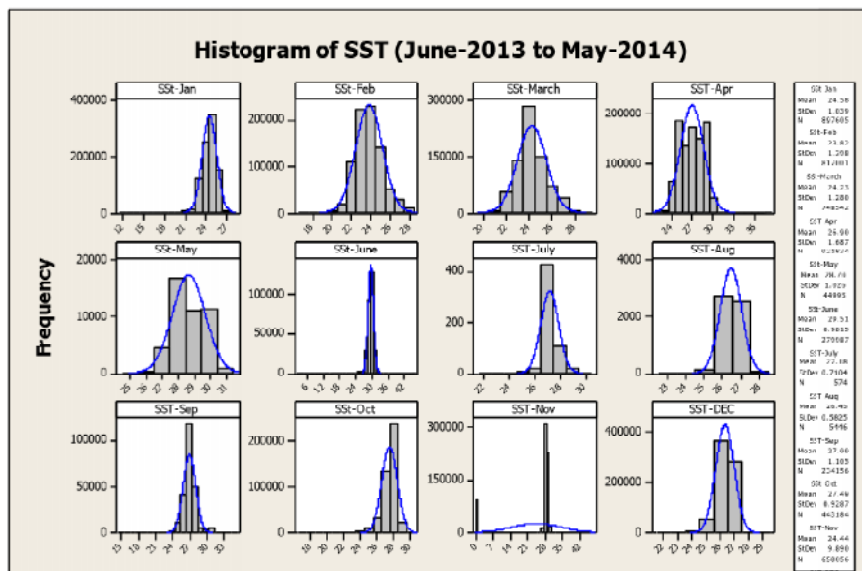


Fig. 4. Histogram of Sea Surface Temperature.

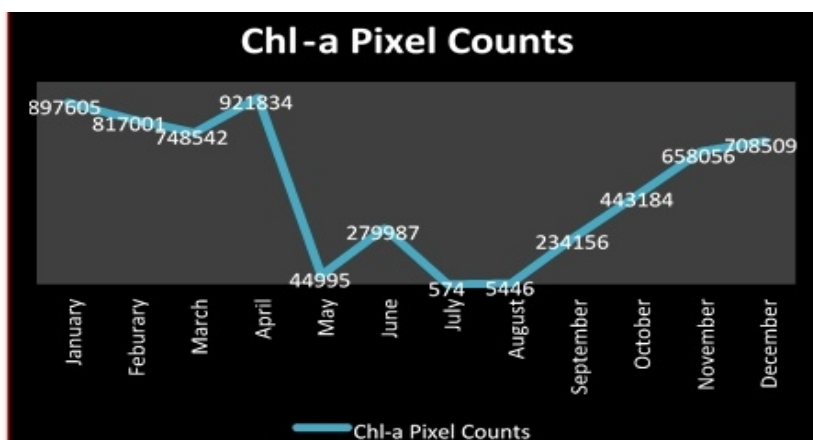


Fig. 5. Chlorophyll-a (Pixel counts).

B. Relationship of Chl-a and SST

For correlating Chl-a and SST pixel values are extracted and analyzed in Minitab statistical software and the relationship has calculated based on monthly data of June 2013 to May 2014.

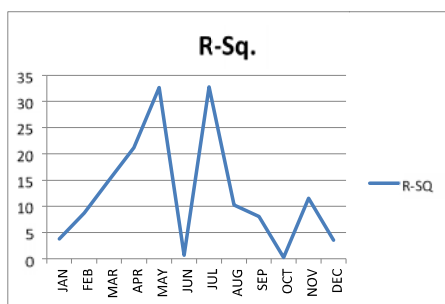


Fig. 6. R-Sq.

There is a statistically significant relationship is found in between SST and Chl-a. In addition RSq is variable from month to month (Fig. 6 and 7).

C. Distribution of Chlorophyll-a pigment concentrations

A pattern of chlorophyll-a concentration evenly distributed in all over the sea during winter months and the value ranging between the 0.031 to 0.432 mg m³. The broad distribution of the chlorophyll-a concentrations higher than 0.194 mg m³ extending Northeastern and southeastern part of the sea during January, as well as in February, the pigment concentrations higher than 0.218 in North central, central, and southern part of the sea whereas, in March the concentrations lower than 0.123 mg m³ (Fig. 8). The red color box represent highest chlorophyll-a concentration on the map.

The pigment concentrations higher than 1.689 mg m⁻³ in the southern and southwest (coast of Yemen) and southeast region of the Arabian Sea in month of April (Fig. 8). The highest value of chlorophyll-*a* concentrations observed during this month range between 2.77 to 4.70 mg m⁻³. During the month of May, pigment concentrations are low over the Arabian

Sea, only southern and northeast part of the sea where the distribution of pigment concentrations higher than 0.158 mg m⁻³ (Fig. 9). In the month of June, the broad distribution of pigment concentrations are found over the north eastern and southeastern region of the sea, as well as few concentrations are found along the Yemen coast.

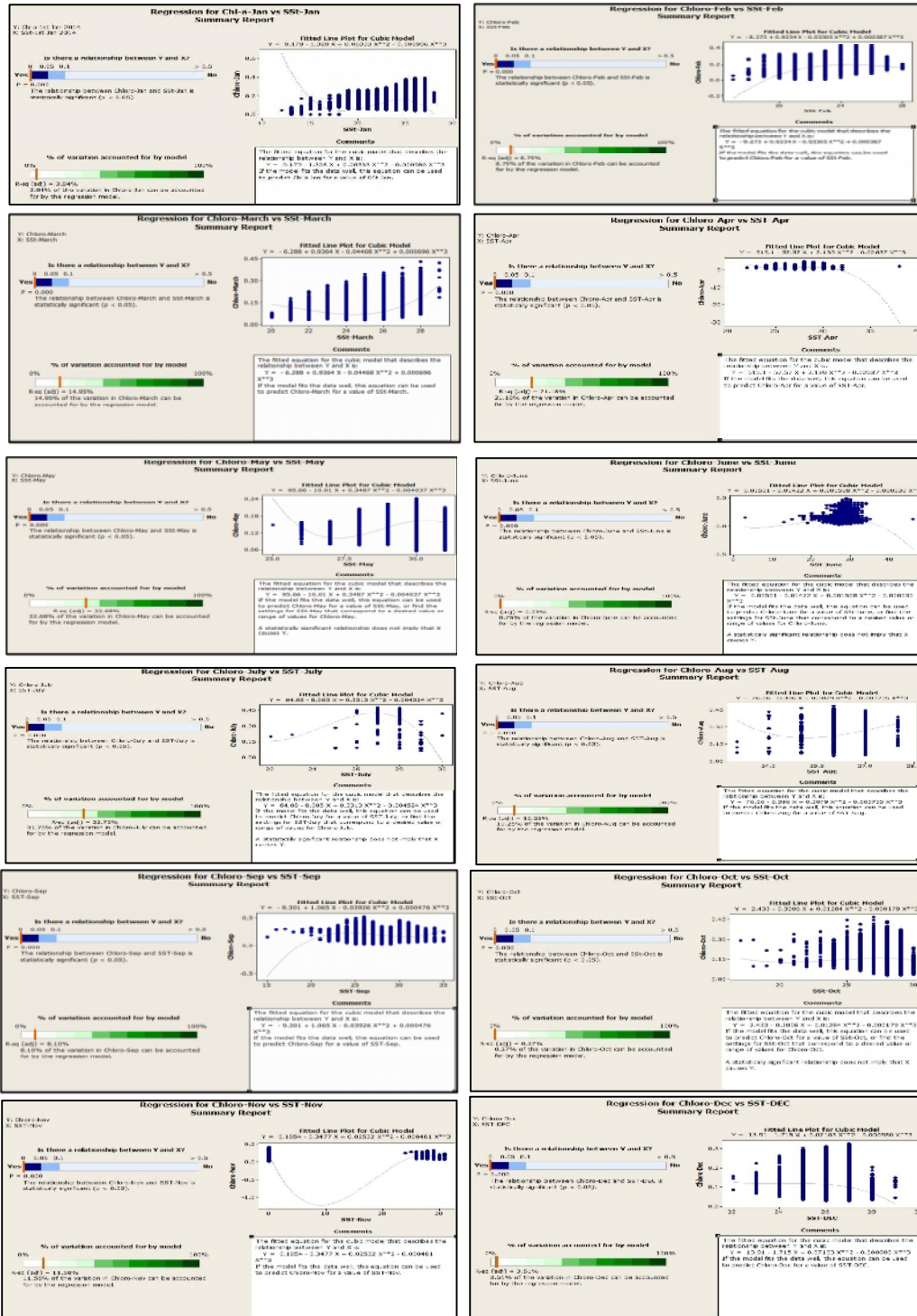


Fig. 7. Regression analysis for chlorophyll vs SST (January to December).

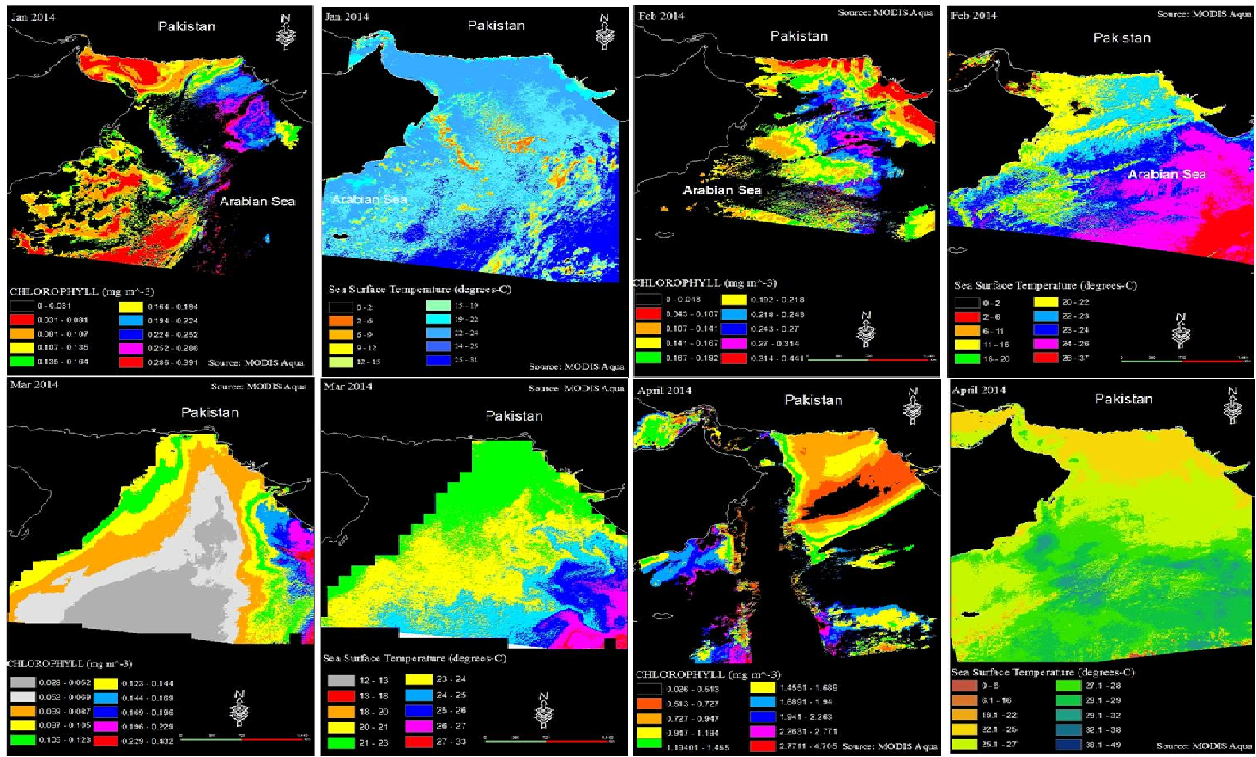


Fig. 8. Chlorophyll-a and SST distribution on Arabian Sea.

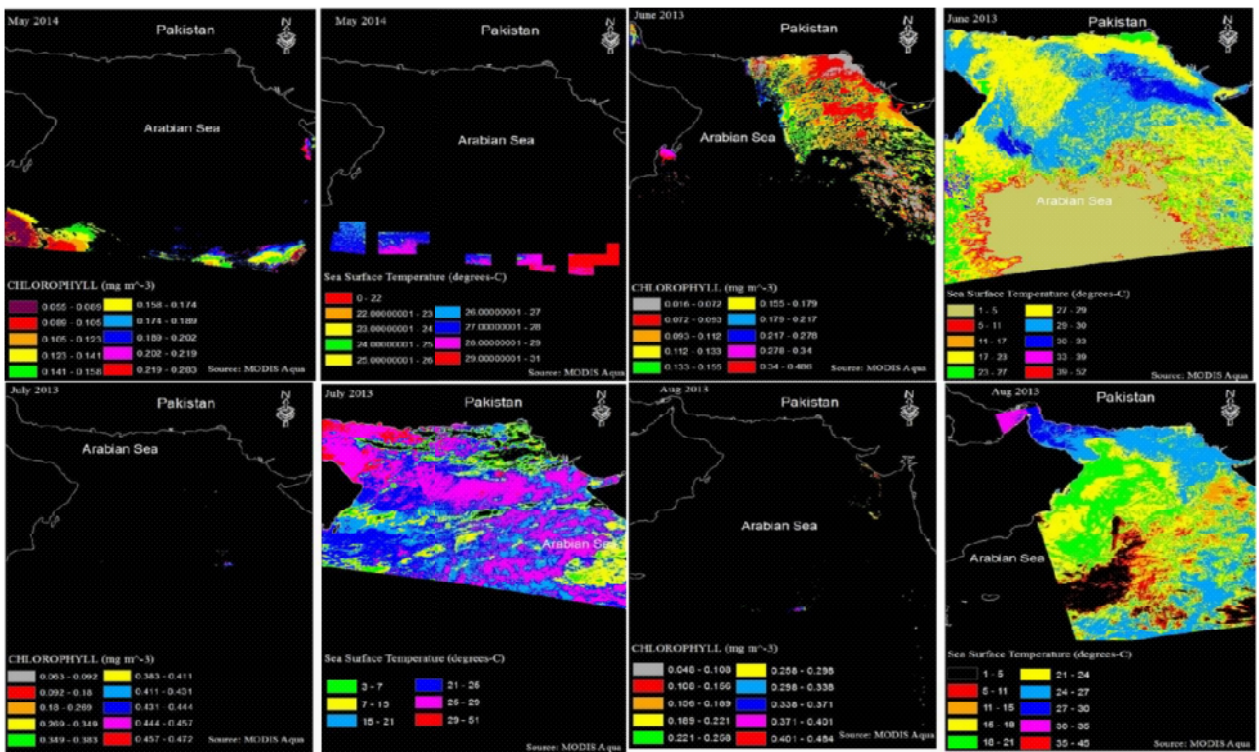


Fig. 9. Chlorophyll-a and SST distribution on Arabian Sea.

The very few pigment concentrations observed in the month of June and August (Fig. 9). The scattered pigment concentration found in south and western part of the Arabian Sea. In month of September, high pigment concentrations occur again in the Arabian Sea, the isolated distribution of the chlorophyll-*a* concentration higher than 0.258 mg m³ (appears along the gulf of Oman, Yemen coast and southern and central part of the Arabian Sea) (Fig. 10). The Chl-*a*

concentrations found all over the sea except the gulf coast and Oman coast during the month of October. The value range between in this month is 0.029 to 0.466 mg m³. In November, the pigment concentrations higher than 0.19 mg m³ in northwest and southwest region. The Chl-*a* concentrations found in all over the sea in December where the broad distribution of concentrations higher than 0.137 mg m³ (Fig. 10).

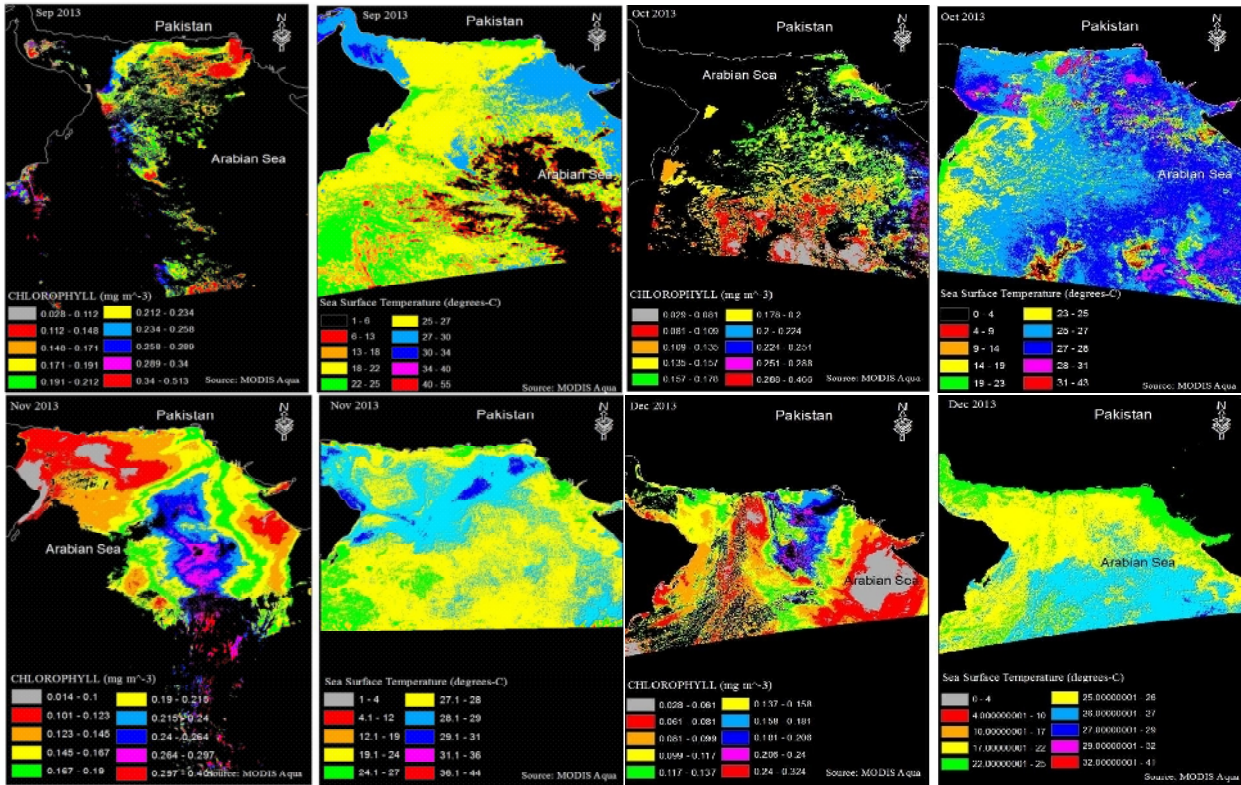


Fig. 10. Chlorophyll-*a* and SST distribution on Arabian Sea.

D. Distribution of Sea Surface Temperature (SST)

The SST maps are shown in Fig.8, 9, and 10. The monthly image analysis show that there is a fluctuations in spatial distribution of SST over Arabian Sea. In the month of January the spatial variation of SST appears in the sea, the temperature value ranged between 2 to 31°C. During this month, the temperature between 19 to 31°C all over the Arabian Sea, only few patches has observed temperature from 2 to 9°C. SST are low (19-22°C) on the southwest to northeastward part (Fig. 8) while, the SST values from 24-25°C on the north, Northwest, west, and southwest part of the sea (Coast from India, Pakistan, Iran, gulf, Oman, and Yemen). The south and southeast region has high temperature ranged from 25-31°C. SST is high (23-37°C) on the southeast part than the northwest part with an area of low SST (16-22°C) during February. The month of March, SST range between 21 to 27°C whereas, the most of the Arabian Sea SST is between 21 to 24°C.

The SST ranged from 16 to 38°C in April and the offshore area of India, Pakistan and the gulf have low temperature (16-22°C) while, temperature observed from 25-28°C on the rest of the sea except some patches in southeast and western part (32-38°C). May SST is 27-31°C in southern part of the sea. A very high spatial variation of SST observed in the month of June. The SST is lowest on the southern part than in the northern part (17-33°C) with a distinct area of low Sea surface Temperature (1-5°C). Maximum SST temperature observed (29-51°C) in the month of July on gulf coast while, the rest of the region SST is 15-29°C except the southeast region where the SST is 7-15°C. The SST is gradually decreases from the gulf coast to Indian coast and then all over the Arabian Sea (1 to 35°C) in August, except the southeastern part of the where the temperature is ranged between 35 to 45°C. The most of the Arabian sea SST is 22 to 27°C in September.

The temperature is 27 to 30°C on the gulf coast and Indian coast whereas, two patches on gulf SST is 30-34°C can be seen in Fig. 10. In the southeastern side of the sea the lowest SST observed between 1-6°C while some patches of highest SST found (40-55°C) on south and southeast part of the sea, therefore the great spatial variation of SST can be seen in this month. October SST values relatively uniform (25-28°C) on entire sea only some scatter patches values 28-31°C in some part of the sea while, the coast of Oman and Yemen SST is 19-23°C. The November sea surface temperature value found from 27 to 31°C over all over the sea where, most of the region SST are 27 to 28°C. The SST along the gulf, Pakistan, and Indian coast are 22 to 25°C in December. The southern part of the sea has 26 to 27°C SST as well as the north, northeast, and southwest part have 25-26°C.

CONCLUSION

The present study illustrates the Monthly variation of Chlorophyll-*a* concentration and association with SST in Arabian Sea. Significant correlation between Sea surface temperature and Chl-*a* concentration were also obtained. The study of Chl-*a* concentration showed that the period of high Chl-*a* concentration found from September to February with a peak in November. A period of low Chl-*a* concentration are found in May to August. The seasonal variation in chlorophyll-*a* concentration was highest in autumn and winter and lowest in summer. The study also revealed that the maximum SST observed in month of September and the minimum is observed in the month of June, August, and September. The distribution of lowest SST observed in the south and southeastern part of the Arabian Sea.

REFERENCES

- Banase, K., & English, D. (2000). Geographical differences in seasonality of CZCS-derived phytoplankton pigment in the Arabian Sea for 1978-1986. *Deep Sea Research Part II: Topical Studies in Oceanography*, **47**(7), 1623-1677.
- Behrenfeld, M. J., O'Malley, R. T., Siegel, D. A., McClain, C. R., Sarmiento, J. L., Feldman, G. C., . . . Boss, E. S. (2006). Climate-driven trends in contemporary ocean productivity. *Nature*, **444**(7120), 752-755.
- Bhattathiri, P., Pant, A., Sawant, S., Gauns, M., Matondkar, S., & Mahanraju, R. (1996). Phytoplankton production and chlorophyll distribution in the eastern and central Arabian Sea in 1994-1995. *Current Science*, **71**, 857-862p.
- Boyce, D. G., Lewis, M. R., & Worm, B. (2010). Global phytoplankton decline over the past century. *Nature*, **466**(7306), 591-596.
- Clark, D. K. (1981). Phytoplankton pigment algorithms for the Nimbus-7 CZCS, in *Oceanography from Space* (J. F. R. Gower, Ed. ed., pp. 227-237). Plenum, New York.
- Doney, S. C. (2006). Oceanography: Plankton in a warmer world. *Nature*, **444**(7120), 695-696.
- Gordon, H. R., Clark, D. K., Brown, J. W., Brown, O. B., Evans, R. H., & Broenkow, W. W. (1983). Phytoplankton pigment concentration in the Middle Atlantic Bight: Comparison of ship determinations and CZCS estimates. *Appl. Opt.*, **22**, 20-36.
- Hayward, T., & Venrick, E. (1982). Relation between surface chlorophyll, integrated chlorophyll and integrated primary production. *Marine Biology*, **69**(3), 247-252.
- Lévy, M., Shankar, D., André, J.M., Shenoi, S. S. C., Durand, F., & Montégut, C. d. B. (2007). Basin-wide seasonal evolution of the Indian Ocean's phytoplankton blooms. *J. Geophys. Res.*, **112**, C12014.
- Li, H.P., Gong, G.C., & Hsiung, T.M. (2002). Phytoplankton pigment analysis by HPLC and its application in algal community investigations. *Botanical Bulletin of Academia Sinica*, **43**.
- Longhurst, A. R. (1998). *Ecological Geography of the Sea*. London: Academic Press.
- Piontkovski, S., & Castellani, C. (2009). Long-term declining trend of zooplankton biomass in the Tropical Atlantic. *Hydrobiologia*, **632**(1), 365-370.
- Varkey, M. J., Murty, V. S. N. A., & Suryanarayana, A. (1996). Physical Oceanography of the Bay of Bengal and Andaman Sea. *Oceanography and Marine Biology: an Annual Reviews*(eds): A.D. Ansail, R.N. Gibson and Margaret Barnes. **34**, 1-70.
- Wiggert, J., Hood, R., Banase, K., & Kindle, J. (2005). Monsoon-driven biogeochemical processes in the Arabian Sea. *Progress in Oceanography*, **65**(2), 176-213.
- Worm, B., Sandow, M., Oschlies, A., Lotze, H. K., & Myers, R. A. (2005). Global patterns of predator diversity in the open oceans. *Science*, **309**(5739), 1365-1369.